SPECTRUMASTRO

SPECTRUM ASTRO, INC.

HIGH ENERGY SOLAR SPECTROSCOPIC IMAGER (HESSI) PROGRAM

ATTITUDE CONTROL SUBSYSTEM

FLIGHT SOFTWARE SPECIFICATION

CONTRACT NO. PPB005884

PREPARED BY:
SPECTRUM ASTRO, INC.
1440 N. Fiesta Boulevard
Gilbert, Arizona 85233
CAGE Code 0T9D1

INITIAL RELEASE DATE
2 SEPTEMBER 1999

SPECTRUM ASTRO, INC.

HIGH ENERGY SOLAR SPECTROSCOPIC IMAGER (HESSI) PROGRAM

ATTITUDE CONTROL SUBSYSTEM

FLIGHT SOFTWARE SPECIFICATION)

CONTRACT NO. PPB005884

REVIEWED BY: _____
CONFIGURATION/DATA CONTROL, DAVE MAIDEN DATE

PREPARED BY: _____
ENGINEERING, GLENN CREAMER DATE

APPROVED BY: _____
QUALITY ASSURANCE, JEFF SQUIRES DATE

APPROVED BY: _____
SYSTEMS ENGINEERING, JOHN JORDAN DATE

APPROVED BY: _____
PROGRAM MANAGER, JEFF PREBLE DATE

REVISION SUMMARY

REV	RELEASE DATE	BRIEF DESCRIPTION/REASON FOR CHANGE	EFFECTIVE PAGES
-	2 September 1999	Initial release.	All

LIST OF ABBREVIATIONS AND ACRONYMS

ACS	Attitude Control Subsystem
ADP	Acceptance Data Package
CBE	Current Best Estimate
CDHS	Command and Data Handling Subsystem
CPU	Central Processing Unit
FOV	Field of View
HESSI	High Energy Solar Spectroscopic Imager
IAD	Inertia Adjustment Device
IDPU	Instrument Data Processing Unit
LV	Launch Vehicle
MAG	Three-Axis Magnetometer
PACI	Payload and Attitude Control Interface
PFS	Product Function Specification
RAS	Roll Angle Sensor
RPM	Revolutions Per Minute
S/C	Spacecraft
SAS	Solar Aspect System
SMS	Structures and Mechanisms Subsystem
SPI	Sun Presence Indicator
TQR	Torque Rod

TABLE OF CONTENTS

TABLE OF CONTENTS (CONTINUED)

PAGE

LIST OF FIGURES

LIST OF TABLES

1. INTRODUCTION

1.1 Scope

This specification establishes the design and algorithm development of the Attitude Control Subsystem (ACS) as implemented on the High Energy Solar Spectroscopic Imager (HESSI) spacecraft. The specification encompasses all modes of operation for the spacecraft, transition logic between modes, sensor processing, on-orbit balancing, uplinkable command parameters, and hardware and software telemetry points. This specification is proprietary to Spectrum Astro, Inc.

1.2 Classification

This document is UNCLASSIFIED.

2. APPLICABLE DOCUMENTS

No additional documents are referenced in this specification.

3. HESSI SPACECRAFT DEFINITION AND MISSION REQUIREMENTS

The HESSI spacecraft and its mission are briefly described in this section, with emphasis on the ACS components and specifications. The description includes component identification and layout, coordinate frames, on-orbit configuration and parameters, and control objectives and requirements.

3.1 Spacecraft Description

The HESSI spacecraft, depicted in Figure 3-1, is composed of a primary truss structure housing a cylindrical scientific imager, four solar arrays extending from the structure, and a variety of subsystem components attached within the structure shell. The entire bus is spin-stabilized about the imager (Z_B) axis at 15 RPM to achieve dynamic stiffness. The solar arrays along the positive X_B and Y_B axes possess on-orbit angular adjustment capability using Inertia Adjustment Devices (IAD) at their root to minimize products of inertia. The ACS hardware suite consists of eight Coarse Sun Sensors (CSS) with two located at the ends of each array, one Fine Sun Sensor (FSS) located at the front of the Imager, one Three-Axis Magnetometer (MAG) located on the $-X_B$ face of the structure, and three Electromagnetic Torque Rods (TQR) located along the X_B, Y_B, and Z_B directions. The scientific imager contains a Solar Aspect System (SAS) which provides Sun vector information and a Roll Angle Sensor (RAS) which provides phase angle information about the spin axis. The ACS utilizes the SAS output as a backup sensor in the event of FSS failure and as a primary sensor for balancing the spacecraft with the IADs. Each of these components is described in detail in Section 3.3 and in Section 4. Though not formally part of the ACS hardware suite or the flight software, a brief description of the IAD and the on-orbit balancing procedure is provided in Section 5.

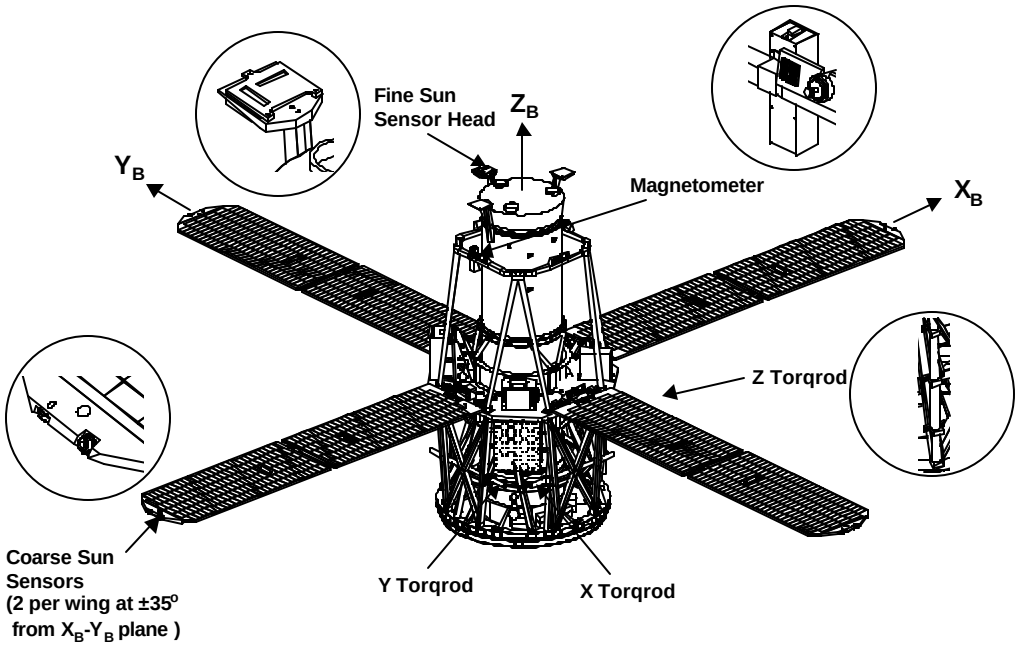

Figure 3-1. HESSI Spacecraft With ACS Components

3.2 ACS-Related Mission Requirements

The nominal HESSI scientific mission is to study the physics of solar flares over a two-year period. This will be achieved by pointing the Solar Spectroscopic Imager towards the Sun using the torqrods to reject both on-board and environmental disturbances as well as to track the 1 degree/day relative motion of the Sun line, as depicted by the on-orbit configuration in Figure 3-2. The primary ACS-related mission requirements, provided in Table 3-1, are to limit pointing errors to 0.2 degrees and maintain a spin rate of 13 to 17 RPM with a rate stability of less than 180 arcseconds in 10 revolutions. The ACS must also be capable of establishing Sun acquisition from any initial orientation upon launch vehicle separation.

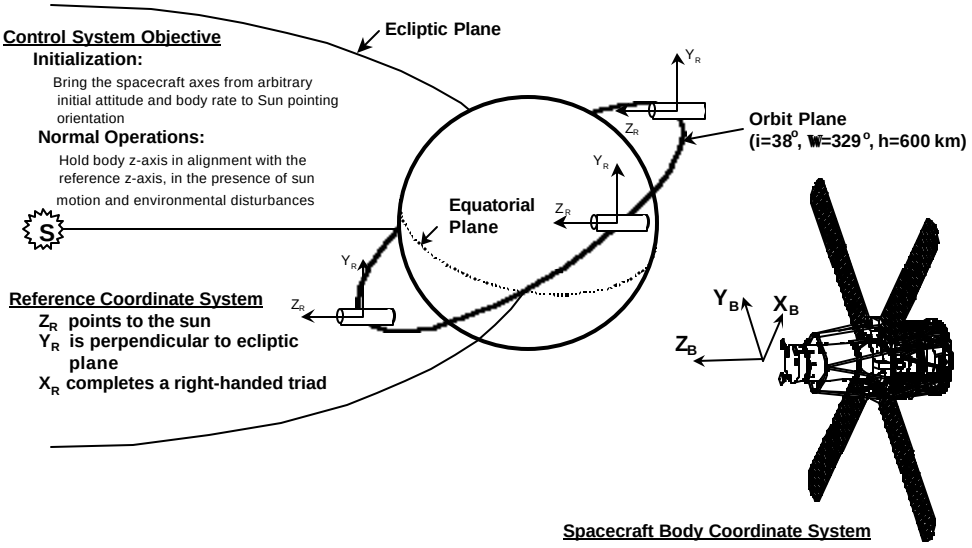

Figure 3-2. On-Orbit Configuration

Table 3-1. ACS-Related Mission Requirements

			Requirement Traceability		
Parameter	**Requirement**	**Capability**	**Source**	**Implementation**	**Verification Method**
Spacecraft Attitude Stabilization	Spin stabilized	Comply	System Specification	ACS	Operation
Spacecraft Spin Rate	15 RPM	15 ± 2 RPM	System Specification	ACS	Analysis
Sun Pointing Control	< 0.2 degrees	0.14 degrees	System Specification	ACS, SMS, FSS PFS (#1110-EW-T10163)	Analysis
Spin Rate Stability	180 arcseconds in 10 revs	125 arcseconds in 10 revs while in Sun; default procedure is to control spin rate in eclipse	System Specification	ACS	Analysis
SAS Data Compatibility	SAS data shall be used as back-up for Sun vector estimation	Comply	System Specification	ACS	Operation
Maximum LV Tip-Off Rate	4 deg/sec in transverse axes	6 deg/sec	System Specification	ACS	Analysis
Initial Sun Acquisition	The S/C shall autonomously acquire the Sun from any orientation upon separation from the LV	Comply	System Specification	ACS	Analysis
CSS Sun Vector Measurement Range	The CSS suite shall provide 4π steradian coverage	Comply	System Specification	ACS, SMS, CSS PFS (#1110-EW-T10164)	Analysis

3.3 ACS Sensor/Actuator Suite

As described previously, the ACS hardware suite consists of eight Coarse Sun Sensors, one Fine Sun Sensor, one Three-Axis Magnetometer, three Electromagnetic Torque Rods, and one Solar Aspect System as a backup Sun sensor. The CSS complement provides full 4π steradian coverage of the celestial sphere with a Sun vector accuracy of a few degrees. These sensors are primarily utilized during initial acquisition but may also be used for troubleshooting purposes. The FSS is the primary Sun sensor and is used in normal science-collecting operations and in initial acquisition (once the Sun is within the sensor's 32 degree FOV). The FSS has a 3σ accuracy of 0.05 degrees within a 10 degree cone and 0.1 degrees outside the 10 degree cone. The MAG provides a measure of the local magnetic field in the S/C frame and is used to determine spin rate (from zero crossings of the X or Y components) and to calculate the appropriate dipole moments applied to the torque rods. Its 3σ accuracy is 4 milliGauss with a range of ±600 milliGauss. The three TQRs provide dipole moments on the S/C and, in combination with the Earth's magnetic field, generate desired torque's along each S/C axis. These actuators are used for precession control, nutation control, and spin rate control, and possess a linear dipole capability of 60 Amp-meters^2. The SAS is utilized as a backup Sun sensor in the ACS control loops and provides a 3σ accuracy of about 28 arcseconds within its 1 degree FOV.

The processing algorithms for each of the sensors are described in detail in Section 4. The components, except the SAS, are provided in Table 3-2.

Table 3-2. ACS Equipment List

Subsystem	Component	Supplier	# Per Flight Shipset
ACS	Fine Sun Sensor Head	Adcole	1
	Fine Sun Sensor Electronics	Adcole	1
	Coarse Sun Sensor	Adcole	8

	Magnetometer	Ithaco	1
	Electromagnetic Torque Rod	Ithaco	3

4. SENSOR PROCESSING

The processing algorithms for each ACS sensor are provided in this section. The outputs of these algorithms provide the necessary information which is utilized in the control laws of Section 6 to drive the torque rods and meet the ACS-related mission requirements.

4.1 Three-Axis Magnetometer

The Three-Axis Magnetometer provides a measure of the magnetic field vector in the S/C frame. The magnetometer processing algorithm consists of two components: calculation of the magnetic field and estimation of the S/C spin rate about the Z_B axis.

4.1.1 Magnetic Field Determination

The primary outputs of the MAG are three voltages proportional to the local magnetic field and one voltage proportional to the temperature. The field strength **B** in Teslas is given by

$$\mathbf{B} = \mathbf{A} * \mathbf{F} * (\mathbf{V}_B - \mathbf{V}_{bias} - \mathbf{V}_{TQR});$$

$$\mathbf{V}_{TQR} = \mathbf{C}_{TQR}\mathbf{I}_M;$$

where $\mathbf{V}_B$ is the 3×1 vector of field voltages output from the MAG, $\mathbf{V}_{bias}$ is the 3×1 vector of bias voltages, $\mathbf{V}_{TQR}$ is the 3×1 vector of TQR-compensated voltages, **A** is a 3×3 alignment matrix, **F** is a 3×3 diagonal scale factor matrix in Tesla/volts, $\mathbf{C}_{TQR}$ is the 3×3 TQR compensation matrix, and $\mathbf{I}_M$ is the 3×1 vector of commanded TQR currents in amps. The TQR compensation matrix will be calibrated on the ground prior to launch and on-orbit prior to normal operations. The alignment and scale factor matrices will be calibrated by Ithaco and provided in their ADP. The calculated magnetic field **B** is filtered using a digital single-pole low-pass filter, as depicted by the z-domain transform

$$\mathbf{B}_f = \left[\frac{a_{LP\_MAG}hz}{(1+a_{LP\_MAG}h)z-1}\right]\mathbf{B};$$

where $\mathbf{B}_f$ is the 3×1 vector of filtered MAG outputs in Teslas, a_{LP_MAG} is the low-pass roll-off frequency in rad/sec, and h is the ACS sample period corresponding to the 8 Hz PACI sampling rate. The value for the roll-off frequency is chosen to be ten times higher than the spin rate of the spacecraft.

4.1.2 Spin Rate Estimation

Estimation of the spin rate about the Z_B axis is achieved by evaluating the zero crossing times of the X and Y components of the MAG output, as follows

If $\text{sign}(B_{xf}) \neq \text{sign}(B_{xf\_old})$

$$t_{cross} = t_c - \frac{B_{xf} h}{B_{xf} - B_{xf\_old}};$$

$$\hat{\Omega}_x = \frac{p}{t_{cross} - t_{cross\_old}};$$

$$t_{cross\_old} = t_{cross};$$

End

where $\hat{\Omega}_x$ is the estimated spin rate from B_{xf} in rad/sec, t_c is the current time, t_{cross} is the interpolated zero cross-over time, and t_{cross_old} is the previous zero cross-over time (one period earlier) The value of B_{xf} – old is set to the most recent value of B_{xf} at the end of each sampling cycle.. The final spin rate estimate $\hat{\Omega}$ is determined from an average of the x and y estimates.

4.2 Coarse Sun Sensors

The Coarse Sun Sensors provide an estimate of the Sun vector in the S/C frame. Each sensor is simply a passive detector which outputs a current proportional to the cosine of the angle between the Sun and the sensor boresight. Therefore, each illuminated sensor gives the location of the Sun on a cone and at least three sensors need to be illuminated to uniquely determine the Sun vector. Since Earth albedo can be as high as 37% of full Sun at the 38 degree orbit plane inclination, its effect needs to be minimized by thresholding the current output of the sensors. The maximum output of each sensor is about 1.3 milli-amps when pointed directly at the Sun; hence, a threshold of 0.45 milli-amps limits the output to 34% of full Sun (corresponding to a FOV threshold of about 70 degrees). The sensor coverage for a 70 degree threshold is shown in Figure 4-1, where it is observed that full 4π steradian coverage is achieved. Although some regions provide only two-sensor coverage (and therefore no unique solution) the calculated Sun vector will still be approximately correct and will direct the S/C in the proper direction until three- or four-sensor coverage is obtained. If the 70 degree cone limit is reduced to 67 degrees (0.5 milli-amps or 39% of full Sun) small regions of one-sensor coverage appear. Again, these regions are not detrimental to the control performance.

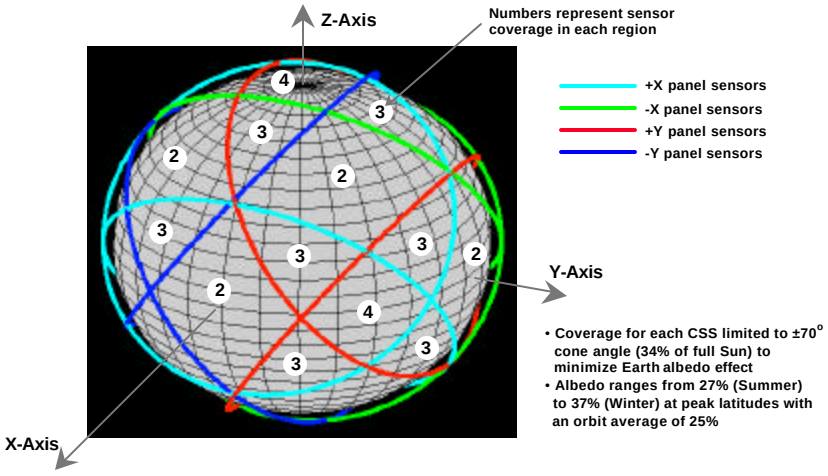

Figure 4-1. CSS Coverage for a 70 Degree Cone Angle Threshold

The CSS processing logic implements the following algorithm

$(SPI)_{CSS} = 0;$

k = 0;

For i = 1:8

If $I_i > I_{threshold}$

$(SPI)_{CSS} = 1;$

k = k+1;

$\mathbf{n}_k = \mathbf{n}_i;$

$I_k = I_i;$

End

End

If k == 1

$\mathbf{S}_{CSS} = \mathbf{n}_1;$

Elseif k == 2

$$\mathbf{S}_{CSS} = S_1 \frac{\mathbf{n}_2 \times \mathbf{n}_1}{|\mathbf{n}_2 \times \mathbf{n}_1|} + S_2 \frac{\mathbf{n}_1 + \mathbf{n}_2}{|\mathbf{n}_1 + \mathbf{n}_2|} + S_3 \frac{\mathbf{n}_1 - \mathbf{n}_2}{|\mathbf{n}_1 - \mathbf{n}_2|};$$

$$S_3 = \frac{I_1 - I_2}{2\sin(\varphi)} \frac{1}{sf_{CSS}};$$

$$S_2 = \frac{I_1 + I_2}{2\cos(\varphi)} \frac{1}{sf_{CSS}};$$

$$S_1 = \pm\sqrt{1 - S_2^2 - S_3^2}\ ;$$

$$\varphi = \frac{1}{2}\cos^{-1}(\mathbf{n}_1 \cdot \mathbf{n}_2)\ ;$$

Elseif k == 3

$$\mathbf{S}_{CSS} = \begin{bmatrix} n_{1x} & n_{1y} & n_{1z} \\ n_{2x} & n_{2y} & n_{2z} \\ n_{3x} & n_{3y} & n_{3z} \end{bmatrix}^{-1} \begin{Bmatrix} I_1 \\ I_2 \\ I_3 \end{Bmatrix} \frac{1}{sf_{CSS}}\ ;$$

Else

$$\mathbf{S}_{CSS} = (\mathbf{A}^T\mathbf{A})^{-1}\mathbf{A}^T \begin{Bmatrix} I_1 \\ I_2 \\ I_3 \\ I_4 \end{Bmatrix} \frac{1}{sf_{CSS}} \qquad \mathbf{A} = \begin{bmatrix} n_{1x} & n_{1y} & n_{1z} \\ n_{2x} & n_{2y} & n_{2z} \\ n_{3x} & n_{3y} & n_{3z} \\ n_{4x} & n_{4y} & n_{4z} \end{bmatrix};$$

End

where $\mathbf{S}_{CSS}$ is the unit Sun vector, n_{ix}, n_{iy}, n_{iz} are the components of the unit boresight vector of the (i)th CSS, I_i is the current output of the (i)th CSS in amps, $I_{threshold}$ is the threshold value of current in amps, sf_{CSS} is the CSS scale factor in amps, and $(SPI)_{CSS}$ is a bi-level CSS-based Sun Presence Indicator which is equal to 1 when the Sun is in view and 0 otherwise. For the case in which only 2 sensors are illuminated (k == 2), the two solutions given above are compared to the previous Sun vector and the one closest to the previous solution is chosen.

4.3 Fine Sun Sensor

The Fine Sun Sensor is the primary ACS pointing sensor which provides a measure of the Sun vector in the S/C frame to a 3σ accuracy of 0.05 degrees. The FSS outputs both a coarse 6-bit gray code digital signal and two fine analog sine and cosine signals for each of two solar aspect angles α and β, as defined in Figure 4-2. The coarse digital signal provides the integer value for each aspect angle in 1 degree increments with a range of ±32 degrees. The fine analog signals provide the fractional components of the two angles. The procedure to obtain the two aspect angles and, hence, the unit Sun vector is as follows:

1. Determine the fractional component N_f for each angle from the analog outputs using

$$N_f = \frac{1}{2\pi}\tan^{-1}\left(\frac{V_{sin}}{V_{cos}}\right)$$

where V_{sin} and V_{cos} are the sine and cosine analog voltage outputs.

2. Determine the integer component N_i for each angle from the coarse digital outputs using

$$\begin{aligned} \overline{N}_i &= N_d + 1 \quad \text{if } N_f < 0.25 \\ &= N_d - 1 \quad \text{if } N_f \geq 0.75 \\ &= N_d \quad \text{if } 0.25 \leq N_f < 0.75 \end{aligned}$$

$$N_i = \text{truncate}\left(\frac{\overline{N}_i}{2}\right)$$

where N_d is the decimal equivalent of the 6-bit gray code.

3. Determine the total error for each angle using

$$N_{x,y} = N_i + N_f$$

4. Determine the projections of the Sun vector onto the X and Y axes using

$$X = 0.011N_x - 0.176$$
$$Y = 0.011N_y - 0.176$$

5. Determine the two aspect angles using

$$\alpha = \tan^{-1}\left(\frac{1.4553X}{\sqrt{0.202644 - 1.117898(X^2 + Y^2)}}\right) + \alpha_0$$

$$\beta = \tan^{-1}\left(\frac{1.4553Y}{\sqrt{0.202644 - 1.117898(X^2 + Y^2)}}\right) + \beta_0$$

where α_0 and β_0 are fixed offset angles provided by Adcole.

6. Determine the unit Sun vector using

$$S_{zFSS} = \frac{1}{\sqrt{1+\tan^2(\alpha)+\tan^2(\beta)}}$$
$$S_{xFSS} = S_{zFSS}\tan(\alpha)$$
$$S_{yFSS} = S_{zFSS}\tan(\beta)$$

In addition to the Sun vector outputs, the FSS provides a bi-level Sun Presence Indicator, $(SPI)_{FSS}$, which is equal to 1 when the Sun is in view and 0 otherwise.

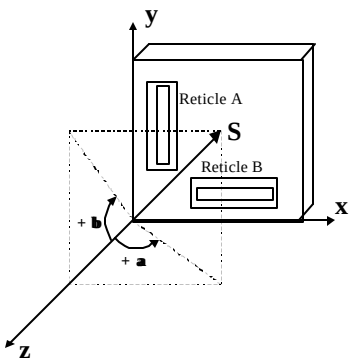

Figure 4-2. FSS Coordinate System and Solar Aspect Angle Definitions

4.4 Solar Aspect System

The Solar Aspect System is the primary sensor utilized during on-orbit balancing operations and the back-up sensor utilized in the event of FSS failure. The SAS output consists of packets of 8 X,Y pairs corresponding to 1 second of Sun vector information sampled at the IDPU rate of 8 Hz. The 1-second intervals are synchronized to the PACI 1 Hz clock. The packets are sent through a serial interface to the PACI with a 1-second delay and are read by the PACI in 0.5 seconds. Therefore, the total delay from the first X,Y pair to the current S/C time is 2.5 seconds.

The propagation logic transfers the 8 pairs of x,y counts to current S/C time and converts the counts to an equivalent Sun unit vector. The counts range from –128 to +127 with a conversion from counts to degrees of 1/128 degrees per count (±1 degree FOV). An output of X=-128 or Y=-128 indicates no solution. The propagation logic is as follows

For i=1:8

If X_i ==-128 **OR** Y_i ==-128

$(SPI)_{SAS\_i} = 0;$

Else

$S_{xSAS\_i} = [X_i \cos(\hat{\Omega}\Delta T) + Y_i \sin(\hat{\Omega}\Delta T)]/128 * (\pi/180);$

$$S_{ySAS\_i} = [Y_i \cos(\hat{\Omega}\Delta T) - X_i \sin(\hat{\Omega}\Delta T)]/128 * (\pi/180);$$

$$S_{zSAS\_i} = \sqrt{1 - S^2_{xSAS\_i} - S^2_{ySAS\_i}}$$

$$(SPI)_{SAS\_i} = 1;$$

End

End

where X_i and Y_i are the (i)th pair of outputs from the SAS in counts, S_{xSAS_i}, S_{ySAS_i}, and S_{zSAS_i} are the (i)th propagated components of the unit Sun vector in radians, $(SPI)_{SAS\_i}$ is the (i)th bi-level SAS-based Sun Presence Indicator, and ΔT is the SAS processing delay in seconds.

5. MODES OF OPERATION

The five modes of operation for the HESSI spacecraft are briefly described in this Section. The modes and their transition paths are depicted in Figure 5-1 and the hardware utilization for each mode is provided in Table 5-1. The specific algorithms associated with each mode are described in detail in Section 6, as well as the transition logic between modes.

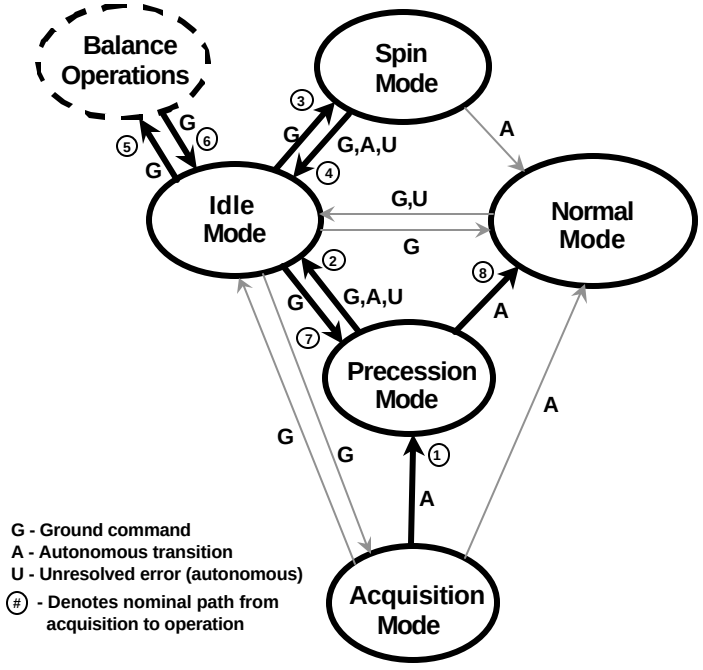

Figure 5-1. Mode Definitions and Transitions

Table 5-1. ACS Hardware Utilization

	Acquisition	Precession	Spin	Normal	Idle	Balance
Spin-Axis TQR	Y	Y	Y	Y (pointing)	On Request	N
Transverse TQR	Y	N	Y	Y (spin rate)	On Request	N
CSS	N	Y	N	N	On Request	N
FSS	N	Y	Y	Y	On Request	Y
MAG	Y	Y	Y	Y	On Request	N
IAD	N	N	N	N	N	Y
SAS	N	Back-Up To FSS	Back-Up To FSS	Back-Up To FSS	On Request	Y

5.1 Acquisition Mode

The Acquisition Mode is the initial wake-up mode entered after release from the launch vehicle and upon any CPU reboots during the mission life. After release from the launch vehicle this mode establishes a prescribed slow spin rate about the spacecraft Z_B axis and damps the transverse rates about the other axes utilizing the MAG and TQR. The MAG output is also used to estimate the spin rate upon entering this mode and determine if the mode was entered from launch vehicle release or from a CPU reboot. If a reboot has occurred then the spin rate will be much higher than the initial 3 deg/sec release rate and will result in a transition to Normal Mode.

5.2 Precession Mode

The Precession Mode can be entered autonomously from Acquisition Mode and by ground command from Idle Mode. This mode establishes a Sun-pointing orientation from any initial attitude to within a fraction of a degree utilizing the CSS, FSS, MAG, and TQR.

5.3 Spin Mode

The Spin Mode is entered only by ground command from Idle Mode. This mode establishes the desired spin rate of 15 RPM while maintaining Sun-pointing orientation utilizing the FSS, MAG, and TQR.

5.4 Normal Mode

The Normal Mode is the primary science-collecting mode of operation and can be entered autonomously from Acquisition Mode, Precession Mode, or Spin Mode and by ground command from Idle Mode. This mode maintains a Sun-pointing accuracy of 0.2 degrees and a spin rate of 13 to 17 RPM utilizing the FSS, MAG, and TQR. Any unresolved pointing or spin rate errors within this mode result in a transition to Idle Mode.

5.5 Idle Mode

The Idle Mode is the safe-hold mode for the spacecraft and is reachable by ground command from any other mode. There are also autonomous transitions to this mode from the other modes based on nominal procedures or unresolved errors. Within this mode the torque rods are disabled and the spacecraft attitude/rate state remains approximately inertially-fixed with minor perturbations due to environmental and on-board disturbances. Exit from this mode to any others is by ground command only. Additionally, on-orbit balance operations are performed within this mode.

6. MODE CONTROL LOGIC

The control logic and algorithms for each of the five modes of operation, as well as the transition logic between each mode, are described in detail in this Section. Additionally, a description of the on-orbit balance procedure is provided at the end of the Section.

6.1 Acquisition Mode Control Logic

The Acquisition Mode is utilized to reduce transverse rates and establish a desired spin rate. A modified "B-Dot" control law is implemented wherein $\dot{B}_z$ is driven to zero while $\dot{B}_x$ and $\dot{B}_y$ are driven to appropriate levels corresponding to a desired spin rate about the Z_B axis. The filtered MAG output is further filtered and differentiated using a second-order finite-difference estimator, resulting in a rate-of-change of the magnetic field in the transfer form

$$\dot{\mathbf{B}}_f = \left[\frac{a_{f\_low} z}{(1+a_{f\_low} h)z - 1}\right]\left[\frac{3z^2 - 4z + 1}{2hz^2}\right]\mathbf{B}_f ;$$

where $\dot{\mathbf{B}}_f$ is the 3×1 vector of filtered field rates in Tesla/sec and a_{f_low} is the low-frequency filter roll-off rate in rad/sec. The commanded TQR dipole moments and currents then become

$$\mathbf{M} = -k_A \begin{Bmatrix} \dot{B}_{xf} - \Omega_A B_{yf} \\ \dot{B}_{yf} + \Omega_A B_{xf} \\ \dot{B}_{zf} \end{Bmatrix} \qquad |\mathbf{M}| \le M_{high} ;$$

$$\mathbf{I}_M = sf_{TQR}\mathbf{M} ;$$

where $\mathbf{M}$ is the 3×1 vector of commanded dipole moments in amp-m^2 (restricted to 60 amp-m^2), k_A is the acquisition control gain in amp-m^2-sec/Tesla, Ω_A is the desired acquisition spin rate in rad/sec, sf_{TQR} is the TQR scale factor in amps/amp-m^2, and M_{high} is the high setting for TQR saturation in amp-m^2.

6.2 Precession Mode Control Logic

The Precession Mode is utilized to establish precise Sun pointing from any arbitrary orientation prior to entering Normal Mode or Idle Mode. The control logic is dependent upon the combination of the Sun Presence Indicators from the CSS and the FSS. If $(SPI)_{CSS}$ is 1 and $(SPI)_{FSS}$ is 0 then a coarse CSS-based logic is executed, if $(SPI)_{FSS}$ is 1 then a fine FSS-based logic is executed, and if $(SPI)_{CSS}$ and $(SPI)_{FSS}$ are both 0 then no current is applied to the TQR (S/C is in eclipse).

6.2.1 Coarse Precession Control

The coarse precession control logic utilizes the CSS-measured Sun vector in combination with the rate-damping acquisition logic to precess the spacecraft. The control logic is as follows

If $(SPI)_{CSS} == 1$ **AND** $(SPI)_{FSS} == 0$

$$\mathbf{S} = \mathbf{S}_{CSS};$$

$$\dot{\mathbf{B}}_f = \left[\frac{a_{f\_low} z}{(1 + a_{f\_low} h)z - 1}\right]\left[\frac{3z^2 - 4z + 1}{2hz^2}\right]\mathbf{B}_f;$$

$$\mathbf{M} = -k_A \begin{Bmatrix} 0 \\ 0 \\ \dot{B}_{zf} \end{Bmatrix} + k_{P\_CSS} \begin{Bmatrix} 0 \\ 0 \\ \text{sign}(B_{xf} S_y - B_{yf} S_x) \end{Bmatrix} \qquad |\mathbf{M}| \le M_{high};$$

$$\mathbf{I}_M = sf_{TQR}\mathbf{M};$$

End

where **S** is the measured Sun vector, and k_{P_CSS} is the CSS precession control gain in amp-m^2.

6.2.2 Fine Precession Control

The fine precession control logic utilizes the FSS-measured Sun vector and the Z_B torque rod to precess the spacecraft. The logic combines both precession control and active nutation control to drive the transverse components of the Sun vector towards zero until the pointing error reaches a small value (i.e. 0.2 degrees). The active nutation control logic requires an estimate of the transverse S/C rates, which are determined from the filtered and differentiated FSS outputs. The precession/nutation logic is as follows

If $(SPI)_{FSS} == 1$

$$\mathbf{S} = \mathbf{S}_{FSS};$$

$$S_{xf} = \frac{S_{xf\_old} + a_{f\_high} h S_x}{a_{f\_high} h + 1}; \qquad S_{yf} = \frac{S_{yf\_old} + a_{f\_high} h S_y}{a_{f\_high} h + 1};$$

$$\dot{S}_{xf} = \left[\frac{3z^2 - 4z + 1}{2hz^2}\right] S_{xf}; \qquad \dot{S}_{yf} = \left[\frac{3z^2 - 4z + 1}{2hz^2}\right] S_{yf};$$

$$\omega_x = \hat{\Omega} S_{xf} + \dot{S}_{yf}; \qquad \omega_y = \hat{\Omega} S_{yf} - \dot{S}_{xf};$$

$$\omega_{xf} = \frac{\omega_{xf\_old} + a_{f\_low} h \omega_x}{a_{f\_low} h + 1}; \qquad \omega_{yf} = \frac{\omega_{yf\_old} + a_{f\_low} h \omega_y}{a_{f\_low} h + 1};$$

$$\hat{\mathbf{o}} = k_{P\_FSS} \hat{\Omega} \begin{Bmatrix} S_{xf} \\ S_{yf} \end{Bmatrix} - k_{N\_FSS} \begin{Bmatrix} \omega_{xf} \\ \omega_{yf} \end{Bmatrix};$$

$$\theta = \cos^{-1}\frac{B_{xf}S_{xf} + B_{yf}S_{yf}}{\sqrt{(B_{xf}^2 + B_{yf}^2)(S_{xf}^2 + S_{yf}^2)}};$$

$M_x = 0;$

$M_y = 0;$

If $0 \le \theta \le \frac{\pi}{2}$

$$M_z = (\frac{2}{\pi}\theta)\frac{B_{xf}\tau_y - B_{yf}\tau_x}{B_{xf}^2 + B_{yf}^2} \qquad |M_z| \le M_{high};$$

Else

$$M_z = (2 - \frac{2}{\pi}\theta)\frac{B_{xf}\tau_y - B_{yf}\tau_x}{B_{xf}^2 + B_{yf}^2} \qquad |M_z| \le M_{high};$$

End

$\mathbf{I}_M = sf_{TQR}\mathbf{M};$

End

where ω_x, ω_y are the transverse rates in rad/sec, a_{f_high} is the high-frequency filter roll-off rate in rad/sec, $\boldsymbol{\tau}$ is the 2×1 torque vector in N-m, k_{P_FSS} is the FSS precession control gain in N-m-sec, k_{N_FSS} is the FSS nutation control gain in N-m-sec, θ is the angle in the X_B, Y_B plane between the Sun vector and the magnetic field, and M_{high} is the high setting for TQR saturation. The "dipole de-weighting" parameter $\frac{2}{\pi}\theta$ scales the control effort depending upon the angle in the x-y plane formed by the B-field vector and the Sun vector.

6.3 Spin Mode Control Logic

The Spin Mode is utilized to establish a desired spin rate about the Z_B axis using the estimated spin rate from the MAG processing output. Simultaneously, the identical fine precession control logic for the Z_B torque rod implemented in the Precession Mode is used to maintain Sun pointing during spin rate correction. The X_B and Y_B torque rod dipole moments and currents are determined using a simple proportional control law with a minimum-norm solution of the form

$$\mathbf{M} = \begin{Bmatrix} k_S\frac{(\Omega_S - \hat{\Omega})}{(B_{xf}^2 + B_{yf}^2)}B_{yf} \\ -k_S\frac{(\Omega_S - \hat{\Omega})}{(B_{xf}^2 + B_{yf}^2)}B_{xf} \\ M_z \end{Bmatrix} \qquad |\mathbf{M}| \le M_{high};$$

$$\mathbf{I}_M = sf_{TQR}\mathbf{M};$$

where k_S is the spin control gain in amp-m^2-Tesla-sec, Ω_S is the desired spin rate in rad/sec, and M_z is the fine precession control dipole given in Section 6.2.2.

6.4 Normal Mode Control Logic

The Normal Mode represents the primary science-collecting mode and requires the tightest pointing accuracy and spin rate stability. Two control functions are performed within this mode: precession/nutation control to maintain the Z_B axis within a deadzone of the Sun line using the Z_B torque rod, and spin rate control to maintain the spin rate within a small deadzone about 15 RPM using the X_B and Y_B torque rods.

6.4.1 Precession/Nutation Control

The precession/nutation control logic is very similar to that described under the Precession Mode logic, with the addition of a pointing hysteresis deadzone. The precession/nutation logic is as follows

If $(SPI)_{FSS} == 1$

$$S_x = S_{xFSS} - S_{xFSS\_bias};$$

$$S_y = S_{yFSS} - S_{yFSS\_bias};$$

$$S_z = \sqrt{1 - S_x^2 - S_y^2};$$

$$S_{xf} = \frac{S_{xf\_old} + a_{f\_high} h S_x}{a_{f\_high} h + 1} \qquad S_{yf} = \frac{S_{yf\_old} + a_{f\_high} h S_y}{a_{f\_high} h + 1};$$

$$\dot{S}_{xf} = \left[\frac{3z^2 - 4z + 1}{2hz^2}\right] S_{xf}; \qquad \dot{S}_{yf} = \left[\frac{3z^2 - 4z + 1}{2hz^2}\right] S_{yf};$$

$$\omega_x = \hat{\Omega} S_{xf} + \dot{S}_{yf} \qquad \omega_y = \hat{\Omega} S_{yf} - \dot{S}_{xf};$$

$$\omega_{xf} = \frac{\omega_{xf\_old} + a_{f\_low} h \omega_x}{a_{f\_low} h + 1} \qquad \omega_{yf} = \frac{\omega_{yf\_old} + a_{f\_low} h \omega_y}{a_{f\_low} h + 1};$$

$$\hat{\mathbf{o}} = k_{P\_FSS} \hat{\Omega} \begin{Bmatrix} S_{xf} \\ S_{yf} \end{Bmatrix} - k_{N\_FSS} \begin{Bmatrix} \omega_{xf} \\ \omega_{yf} \end{Bmatrix};$$

$$\theta = \cos^{-1} \frac{B_{xf} S_{xf} + B_{yf} S_{yf}}{\sqrt{(B_{xf}^2 + B_{yf}^2)(S_{xf}^2 + S_{yf}^2)}};$$

$$\gamma = \cos^{-1}(S_z);$$

$$\gamma_f = \frac{\gamma_{f\_old} + a_{f\_low} h \gamma}{a_{f\_low} h + 1};$$

If $\gamma_f \geq \gamma_{high}$ **OR** $[\gamma_f \geq \gamma_{low}$ **AND** $point\_check == 1]$

point_check=1;

If $0 \leq \theta \leq \frac{\pi}{2}$

$$M_z = (\frac{2}{\pi}\theta)\frac{B_{xf}\tau_y - B_{yf}\tau_x}{B_{xf}^2 + B_{yf}^2} \qquad |M_z| \leq M_{high};$$

Else

$$M_z = (2 - \frac{2}{\pi}\theta)\frac{B_{xf}\tau_y - B_{yf}\tau_x}{B_{xf}^2 + B_{yf}^2} \qquad |M_z| \leq M_{high};$$

End

Else

point_check=0;

$M_z = 0$**;**

End

Else

$M_z = 0$**;**

End

$I_{zM} = sf_{TQR} M_z;$

where $S_{xFSS\_bias}, S_{xFSS\_bias}$ are the bias settings for the FSS, γ is the angle between the Z_B axis and the Sun line, γ_{high} and γ_{low} are the high and low hysteresis bounds on γ, point_check is a bi-level parameter indicating the previous state of the hysteresis loop, and M_{low_P} is the low setting for TQR saturation in precession control in amp-m^2. In the event of FSS failure, the Sun vector and SPI from the SAS will be utilized in place of the corresponding FSS signals.

6.4.2 Spin Rate Control

The spin rate control logic is very similar to that described under the Spin Mode logic, with the addition of a rate hysteresis deadzone. The spin rate logic is as follows

If $\left|\Omega_s - \hat{\Omega}\right| \geq \Delta\Omega_{high}$ **OR** $[\left|\Omega_s - \hat{\Omega}\right| \geq \Delta\Omega_{low}$ **AND** $spin\_check == 1]$

spin_check=1;

$$\begin{Bmatrix} M_x \\ M_y \end{Bmatrix} = \begin{Bmatrix} k_S \dfrac{(\Omega_S - \hat{\Omega})}{(B_{xf}^2 + B_{yf}^2)} B_{yf} \\ -k_S \dfrac{(\Omega_S - \hat{\Omega})}{(B_{xf}^2 + B_{yf}^2)} B_{xf} \end{Bmatrix} \qquad |M_{x,y}| \le M_{low\_S};$$

Else

spin_check=0;

$M_x = 0$**;**

$M_y = 0$**;**

End

$$\begin{Bmatrix} I_{xM} \\ I_{yM} \end{Bmatrix} = sf_{TQR} \begin{Bmatrix} M_x \\ M_y \end{Bmatrix};$$

where $\Delta\Omega_{high}$ and $\Delta\Omega_{low}$ are the high and low hysteresis bounds on $\Delta\Omega$ in rad/sec, spin_check is a bi-level parameter indicating the previous state of the hysteresis loop, and M_{low_S} is the low setting for TQR saturation in spin control in amp-m^2.

6.5 Idle Mode Control Logic

The Idle Mode represents a safe-hold or wait mode with all three torque rods disabled. The commanded TQR dipoles and currents therefore become

$\mathbf{M} = \mathbf{0}$;

$\mathbf{I}_M = \mathbf{0}$;

until ground-command intervention.

6.6 Mode Transition Logic

The transition logic between each mode of operation is outlined in Table 6-1. The left-most column of the table represents the Mode the spacecraft is currently operating within and the upper-most row represents the Mode the spacecraft will transition to if the appropriate block logic is satisfied. For example, if the spacecraft is in Normal Mode, the only possible transition is to Idle Mode if the pointing error between the measured Sun vector and the spacecraft Z_B axis, β, exceeds its allowable bound or if the estimated spin rate, Ω, exceeds its allowable bound. The logic for transition from Acquistion Mode to Precession Mode is based on time from LV release and estimated spin rate. It is also observed that the bounds for transition to Normal Mode from either Precession Mode or Spin Mode must be tighter than the corresponding bounds within Normal Mode or a transition to Idle Mode will immediately occur. If the spacecraft is in Idle Mode, the only transition to any other Mode is through ground command. It should be stated that although the parameters are numerical in Table 6-1, they will actually be variables which can be modified and uploaded at any time during the mission life (see Section 7.1).

Table 6-1. Mode Transition Logic

	Acquisition	***Precession***	***Normal***	***Spin***	***Idle***
Acquisition		Time since LV release > 2.5 hours	β < 5.0 deg AND Ω > 0.12 rpm	None	Ground Command
Precession	None		β < 0.2 deg AND 14.5 < Ω < 15.5 rpm	None	Ground Command OR { β < 5 deg AND NOT 14.5 < Ω < 15.5 rpm }
Normal	None	None		None	Ground Command OR β > 0.5 deg OR NOT 13.5 < Ω < 16.5 rpm
Spin	None	None	14.5 < Ω < 15.5 rpm AND β < 0.2 deg		Ground Command OR { 14.5 < Ω < 15.5 rpm AND NOT β < 0.2 deg }
Idle	Ground Command	Ground Command	Ground Command	Ground Command	

Note: Transition from Acquisition to Normal occurs only if β check is valid continuously for 10 minutes.

6.7 On-Orbit Balance Operations

On-orbit balance operations are performed within Idle Mode after initial Sun acquisition and, if required, periodically during the mission life. The balance procedure is performed entirely by ground command and monitoring and, hence, adds no flight software code to the processor. The procedure utilizes the IAD on each of the two positive-facing X and Y arrays to adjust the angle of the arrays such that the spin axis aligns itself with the HESSI Imager boresight axis. The IAD is a micrometer displacement device with a resolution of 0.00043 cm resulting in a spin axis angle resolution of 0.0022 degrees. Balancing is accomplished by monitoring the SAS Sun vector output on the ground and removing any biases associated with the X and Y components of that vector. The steps associated with this procedure are as follows

1. Calculate the Imager unit Sun vector, $(S_{xSAS}, S_{ySAS}, S_{zSAS})$, from the SAS output
2. Average S_{xSAS} and S_{ySAS} over a short time period to obtain the X,Y biases (b_x, b_y)
3. Calculate the required X,Y array angles, $\theta_{x,y}$, to remove these biases using

$$\theta_{x,y} = \frac{-(I_s - I_t)b_{x,y}}{(m_{array} + m_{tip})(R + \bar{L})\bar{L}}$$

$$\bar{L} = \frac{m_{array}\frac{L}{2} + m_{tip}L}{m_{array} + m_{tip}}$$

where I_s is the spin inertia, I_t is the transverse inertia, L is the length of the array, R is the radius of the cylindrical S/C bus, m_{array} is the mass of the array (minus the tip mass), and m_{tip} is the array tip mass.

4. Determine commanded IAD displacements, $d_{x,y}$, using

$$d_{x,y} = -f\theta_{x,y}$$

where f is the fulcrum arm length of 20.4 cm.

The above steps can be iterated if necessary until the desired balance accuracy is achieved.

7. COMMAND, INTERFACE, AND TELEMETRY PARAMETERS

Provided in this section are the wide range of uplinkable ACS command parameters, ACS flight software interface variables, and ACS downlinkable telemetry parameters. The command parameters can be uplinked as an entire table or, if desired, as a single parameter at a time. The telemetry parameters will be monitored on the ground to assess the on-orbit status and performance of the ACS and to assist in on-orbit troubleshooting.

7.1 ACS Command Parameters

The ACS command parameters are provided in Table 7-1. The table includes launch default values for each parameter. These parameters will be adjustable by ground command throughout the mission. The parameters with an asterisk vary autonomously during mission operation.

Table 7-1. ACS Command Parameters

Parameter	Type	Default Value	Description	Range
MODE_COMMAND*	integer	1	Mode setting	1 - 5
CSS_THRESH	float	0.0005 amps	CSS threshold	0 - 0.001
FSS_BIAS_X	float	0	FSS bias along x-axis	± 1
FSS_BIAS_Y	float	0	FSS bias along y-axis	± 1
MAG_BIAS_X	float	0 tesla	MAG bias along x-axis	± 0.0001
MAG_BIAS_Y	float	0 tesla	MAG bias along y-axis	± 0.0001
SAS_DELAY	float	2.5 sec	SAS data delay	0 - 5.0
TQR_COMP11	float	0 volts/amp	Torque rod compensation matrix component	± 20
TQR_COMP12	float	0 volts/amp	Torque rod compensation matrix component	± 20
TQR_COMP13	float	0 volts/amp	Torque rod compensation matrix component	± 20
TQR_COMP21	float	0 volts/amp	Torque rod compensation matrix component	± 20
TQR_COMP22	float	0 volts/amp	Torque rod compensation matrix component	± 20
TQR_COMP23	float	0 volts/amp	Torque rod compensation matrix component	± 20
TQR_COMP31	float	0 volts/amp	Torque rod compensation matrix component	± 20
TQR_COMP32	float	0 volts/amp	Torque rod compensation matrix component	± 20
TQR_COMP33	float	0 volts/amp	Torque rod compensation matrix component	± 20
TQR_SAT_HIGH	float	60 amp-m ^{2}	Torque rod high saturation level	0 - 100
TQR_SAT_POINT_LOW	float	30 amp-m ^{2}	Torque rod low saturation level in pointing	0 - 100
TQR_SAT_SPIN_LOW	float	10 amp-m ^{2}	Torque rod low saturation level in spin	0 - 100
ACQ_SPIN_COM	float	0.035 rad/sec	Commanded spin rate during Acquisition	0 - 0.1
NORM_SPIN_COM	float	1.57 rad/sec	Commanded spin rate during normal operations	0 - 2
ACQ_GAIN	float	100000000000 amp-m ^{2}-sec/tesla	Acquisition control gain	0 - 1.0e+11
COARSE_PREC_GAIN	float	10000 amp-m^2	Coarse precession control gain	0 - 1.0e+06
FINE_PREC_GAIN	float	1.5 N-m-sec	Fine precession control gain	0 - 5
FINE_NUT_GAIN	float	4.5 N-m-sec	Fine nutation control gain	0 - 20
SPIN_GAIN	float	1 amp-m ^{2}-sec/tesla	Spin control gain	0 - 10
POINT_HIGH	float	0.001745	High setting for pointing hysteresis logic	0 - 0.004
POINT_LOW	float	0.0008725	Low setting for pointing hysteresis logic	0 - 0.002
POINT_CHECK*	integer	1	Initial state of pointing hysteresis logic	0,1
DELTA_SPIN_HIGH	float	0.1 rad/sec	High setting for spin hysteresis logic	0 - 0.4
DELTA_SPIN_LOW	float	0.05 rad/sec	Low setting for spin hysteresis logic	0 - 0.2
SPIN_CHECK*	integer	1	Initial state of spin hysteresis logic	0,1
POINT_ACQ2NORM	float	0.0873	Transition pointing error from Acquisition to Normal	0 - 0.2
POINT_PREC2NORM	float	0.0035	Transition pointing error from Precession to Normal	0 - 0.01
POINT_NORM2IDLE	float	0.0088	Transition pointing error from Normal to Idle	0 - 0.01
POINT_SPIN2NORM	float	0.0035	Transition pointing error from Spin to Normal	0 - 0.01
RATE_ACQ2NORM	float	0.0126 rad/sec	Transition rate from Acquisition to Normal	0 - 0.1
DRATE_PREC2NORM	float	0.05 rad/sec	Transition rate error from Precession to Normal	0 - 0.5
DRATE_NORM2IDLE	float	0.15 rad/sec	Transition rate error from Normal to Idle	0 - 0.5
DRATE_SPIN2NORM	float	0.05 rad/sec	Transition rate error from Spin to Normal	0 - 0.5
TIME_ACQ2NORM	float	600 sec	Transition time from Acquisiton to Normal	0 - 1800
TIME_ACQ2PREC	float	9000 sec	Transition time from Acquisiton to Precession	0 - 11000

7.2 ACS Flight Software Interface Variables

The ACS flight software algorithms described in the previous sections will be converted into flight software C code using the Autocode utility provided with the AC1000 realtime development system (see Section 8). This C code will then be integrated with the remaining CDHS code to generate the complete flight software. Provided in Tables 7-2 and 7-3 are the input/output variables which interface to the CDHS code. Each input and output variable name, type, description, and range are given. The difference between *mode_command* of Table 7-1 and *ground_mode* of Table 7-2 is that *mode_command* simply initializes the mode, whereas *ground_mode* holds the mode until it is reset to zero (its default).

Table 7-2. ACS Flight Software Input Variables

Variable	Type	Description	Range
ground_mode	integer	Ground commanded mode	0-5
sun_sensor_toggle	integer	Sun sensor toggle switch (0=FSS, 1=SAS)	0,1
MAG1	float	MAG x output	± 5 volts
MAG2	float	MAG y output	± 5 volts
MAG3	float	MAG z output	± 5 volts
CSS1	float	CSS1 output	0 - 0.0013 amps
CSS2	float	CSS2 output	0 - 0.0013 amps
CSS3	float	CSS3 output	0 - 0.0013 amps
CSS4	float	CSS4 output	0 - 0.0013 amps
CSS5	float	CSS5 output	0 - 0.0013 amps
CSS6	float	CSS6 output	0 - 0.0013 amps
CSS7	float	CSS7 output	0 - 0.0013 amps
CSS8	float	CSS8 output	0 - 0.0013 amps
coarsex	integer	FSS x-axis coarse data	0-64
coarsey	integer	FSS y-axis coarse data	0-64
sinx	float	FSS x-axis sin of angle	± 5 volts
cosx	float	FSS x-axis cos of angle	± 5 volts
siny	float	FSS y-axis sin of angle	± 5 volts
cosy	float	FSS y-axis cos of angle	± 5 volts
FSS_SPI	integer	FSS Sun Presence Indicator	0,1
SC_time	float	Spacecraft time	0 - 1.0e+08 sec
SASx1	integer	SAS x count 1	± 128
SASx2	integer	SAS x count 2	± 128
SASx3	integer	SAS x count 3	± 128
SASx4	integer	SAS x count 4	± 128
SASx5	integer	SAS x count 5	± 128
SASx6	integer	SAS x count 6	± 128
SASx7	integer	SAS x count 7	± 128
SASx8	integer	SAS x count 8	± 128
SASy1	integer	SAS y count 1	± 128
SASy2	integer	SAS y count 2	± 128
SASy3	integer	SAS y count 3	± 128
SASy4	integer	SAS y count 4	± 128
SASy5	integer	SAS y count 5	± 128
SASy6	integer	SAS y count 6	± 128
SASy7	integer	SAS y count 7	± 128
SASy8	integer	SAS y count 8	± 128
SAS_time	float	SAS time tag	0 - 1.0e+08 sec

Table 7-3. ACS Flight Software Output Variables

Variable	Type	Description	Range
Ix	float	Current to TORX	± 0.25 amp
Iy	float	Current to TORY	± 0.25 amp
Iz	float	Current to TORZ	± 0.25 amp
spin_rate_est	float	Spin rate estimate	± 2 rad/sec
mode	integer	Mode	0 - 5
MAGx	float	Magnetic field along x-axis	± 0.0001 tesla
MAGy	float	Magnetic field along y-axis	± 0.0001 tesla
MAGz	float	Magnetic field along z-axis	± 0.0001 tesla
CSSx	float	CSS Sun vector along x-axis	± 1
CSSy	float	CSS Sun vector along y-axis	± 1
CSSz	float	CSS Sun vector along z-axis	± 1
FSSx	float	FSS Sun vector along x-axis	± 1
FSSy	float	FSS Sun vector along y-axis	± 1
FSSz	float	FSS Sun vector along z-axis	± 1
CSS_SPI	integer	CSS Sun Presence Indicator	0,1
wx	float	Transverse rate along x-axis	± 0.1 rad/sec
wy	float	Transverse rate along y-axis	± 0.1 rad/sec
SASx	float	SAS Sun vector along x-axis	± 1
SASy	float	SAS Sun vector along y-axis	± 1
SASz	float	SAS Sun vector along z-axis	± 1
SAS_SPI	integer	SAS Sun Presence Indicator	0,1
to_idle_flag	integer	Flag describing transition to Idle Mode	0 - 5

The *to_idle_flag* variable in Table 7-3 describes why a transition to Idle Mode has occurred. The definitions for this flag are provided in Table 7-4.

Table 7-4. *To_Idle_Flag* Description

to_idle_flag	Description
0	No transition to Idle
1	Not used
2	Precession to Idle: $\beta < 5$ deg AND NOT $14.5 < \Omega < 15.5$ rpm
3	Normal to Idle: $\beta > 0.5$ deg
4	Normal to Idle: NOT $13.5 < \Omega < 16.5$ rpm
5	Spin to Idle: $14.5 < \Omega < 15.5$ rpm AND NOT $\beta < 0.2$ deg

7.3 ACS Telemetry Parameters

The list of ACS telemetry parameters is identical to those 60 variables given in Tables 7-2 and 7-3, with the addition of the FSS state-of-health (FSS_SOH) parameter which is a float value ranging between 0 and 5 volts (with a nominal value of 3.5 volts), and the MAG temperature parameter which is a float value ranging between 0 and 5 volts (with a nominal value of 2.5 volts).